

**Observation of the Tetragonal-Orthorhombic transition in polycrystalline  $\text{YBa}_2\text{Cu}_3\text{O}_{6+\delta}$  samples during the oxidation process at constant temperature via thermogravimetry and differential thermometry analysis**

Lorenzo Gallo,<sup>1</sup> Cesar E. Sobrero,<sup>1,2</sup> Jorge A. Malarría,<sup>1,2</sup> and Roberto F. Lucas<sup>2</sup>

<sup>1</sup>*Universidad Nacional de Rosario, Pellegrini 1120,*

*S2000EZP Rosario, Santa Fé, Argentina.*

<sup>2</sup>*Institute of Physics Rosario, CONICET-UNR,*

*Bv. 27 de Febrero 210bis, S2000EZP Rosario, Santa Fé, Argentina.*

(Dated: May 22, 2024)

## Abstract

This work examines the oxygenation process of polycrystalline powder of  $\text{YBa}_2\text{Cu}_3\text{O}_{6+\delta}$  superconductor material through constant temperature thermogravimetric analysis. Starting from completely deoxygenated samples ( $\delta = 0$ ), both the mass evolution in an oxygen atmosphere and a differential temperature value referenced to an inert sample (alumina powder) subjected to the same experimental conditions are recorded. The oxygenation process itself is identified as an exothermic process accompanied by a second also exothermic associated process. This second process is identified as the Tetragonal-Orthorhombic transition present in the material. Based on the obtained results, the structural phase diagram of the material is reconstructed. Issues of metastability of the structural phases, as well as the potential of the equipment used to obtain these results comparable to those obtained in large facilities, are discussed. Reinterpretations of previously discussed works in the literature are inferred.

## I. INTRODUCTION

The superconductor material  $\text{YBa}_2\text{Cu}_3\text{O}_{6+\delta}$  (YBCO) in its deoxygenated state,  $\delta = 0$ , appears in a Tetragonal phase with identical a and b unit cell parameters[1]. Its typical triple perovskite-like structure is completed with a c parameter value approximately 3 times the a parameter value. This observed symmetry upon 90-degree rotations on the c direction, is broken when the material is oxygenated (where  $0 \leq \delta \leq 1$ ), leading to a transition to an Orthorhombic phase[2, 3].

During oxygenation, the oxygen atoms gained by YBCO are located at the apical sites of the unit cell, at any of the 4 sites the cell has both at its base and its top (base of the next unit cell)[4]. This randomness in the location of absorbed oxygen allows YBCO to maintain its Tetragonal structure at low degrees of oxygenation. As the material oxygenates and the oxygen concentration  $\delta$  increases, the O atoms begin to order, forming Cu-O chains. This results in a preference in the location of oxygen gained by the material, taking the b directions in the a-b plane of the YBCO unit cell. The breaking of this symmetry leads to an expansion of the unit cell in the b direction, resulting in the Tetragonal-Orthorhombic (T-O) transition known in the material[5].

Initially, and considering only the positions that the apical oxygens take in the unit cell, the material undergoes this T-O transition from a disordered phase to an ordered

phase with equal probability of occupation of all apical oxygen sites in the direction of the  $b$  parameter of the unit cell. This order in the Orthorhombic phase is called Ortho-I superstructure; and the T-O transition, known to occur from  $\delta$  values  $\approx 0.5$ , is assumed to this phase with incomplete filling of the available oxygen sites[6–9]. However, it has been measured by high-energy X-ray diffraction experiments[8] that there are different types of superstructures, leading to Orthorhombic phases called Ortho-I, Ortho-II, Ortho-III, Ortho-V, and Ortho-VIII. Among them, the Ortho-I superstructure predominates at both high oxygenation temperatures and high  $\delta$  values, coinciding with being the only one with long-range interaction. Of the remaining superstructures, the one called Ortho-II predominates at low oxygenation temperatures and low  $\delta$  values, coinciding with being the only one with 3D order (like Ortho-I). The other superstructures, found at low oxygenation temperatures and at  $\delta$  values that place them between Ortho-II and Ortho-I phases, are all 2D ordered[8]

In the work presented here, we study the evolution of the mass of YBCO material as a function of oxygenation time  $t_{Oxyg}$  and for different Oxygenation Temperatures  $T_O$  values, in the range of 320°C to 790°C. We work with YBCO powder obtained by grinding superconducting YBCO pellets. The YBCO pellets used were formed from a stoichiometric mixture of oxides of the different compounds that make up the material. The mass variation results during the oxygenation process were obtained with a commercial thermo-gravimetric analysis (TGA) equipment, which also takes data from differential thermometry (DTA) in contrast with an inert sample (alumina powder). Due to the prior treatment the material receives, it is considered that it starts from completely deoxygenated samples, measuring the mass evolution in the complete oxygenation path ranging from  $\delta = 0$  to the value obtained in saturation condition for each  $T_O$ . The results of differential thermometry show the oxygenation of the material as an exothermic process accompanied by a second exothermic process associated with the T-O transition present in the material. In conjunction with the results of thermogravimetry, we observe not only the T-O transition to Ortho-I phase at high  $T_O$  values and to Ortho-II phase at low  $T_O$  values, but also the interface between Ortho-I and Ortho-II superstructures in the Orthorhombic phase, which depends on the material’s oxygenation temperature. We attribute the observation of the interface between superstructures in our experiments at constant  $T_O$ , to both the type of material used and the method employed to conduct our experiments. Both allowing the Tetragonal phase to evolve metastably along this interface. The metastability conditions are discussed in the work. Moreover, the

outstanding potential of the equipment used to obtain results comparable to those obtained in large facilities is also discussed. Additionally, different interpretations of results regarding the theme of oxygenation in the bibliography are proposed.

## II. EXPERIMENTAL DETAILS

We worked with YBCO powder obtained by grinding with an agate mortar of YBCO superconducting samples. The ground samples were sintered from a stoichiometric mixture of powders of the corresponding oxides. A PANalytical Empyrean X-ray diffraction system was used, operating at 40 V and 30 mA and scanning  $2\theta$  angles from 20 to 120 degrees for the study of the obtained powder. X-ray diffraction analysis confirmed the production of YBCO powder in either Tetragonal or Orthorhombic phase depending on the material's degree of oxygenation. An Olympus PME 3 microscope was used, processing the images obtained with TSVIEW software, to determine the grain size of the YBCO powder. Approximately 4.5 g of powder was obtained with a grain size of 5  $\mu\text{m}$ . A Shimadzu DTG-60H TGA was used for TGA and DTA studies. Pt crucibles with a diameter of 6 mm and an alumina powder reference sample within 10% of the material's mass value were used for each measurement. Two different gases were used for the TGA studies: Nitrogen (99.998%(V) min, O<sub>2</sub> 5.00 ppm(V) max, H<sub>2</sub>O 3.00 ppm(V) max) as an inert gas, and Oxygen (99.8%(V) min, H<sub>2</sub>O 10 ppm(V) max). Regardless, an intrinsic error of  $\pm 50 \mu\text{g}$  in the mass reading was observed in the TGA for the temperature range used. Considering a 2.46% increase in the mass of YBCO material for a complete oxygenation (from  $\delta = 0$  to  $\delta = 1$ ), measurements were always made with mass values above 50 mg, with the uncertainty in the mass reading reaching 20% for an oxygenation of only 20% of the total ( $\delta = 0.2$ ) and below 4% for a complete oxygenation ( $\delta = 1$ ). Thus, approximately 55 mg of YBCO powder was used for measurements made in the TGA, always using powder not previously measured.

For X-ray measurements, YBCO powder was used under the same oxygenation conditions as observed in TGA experiments. Three different oxygenation levels were studied: completely deoxygenated ( $\delta = 0$ ), oxygenated at low  $T_O$  (350 °C,  $\delta \approx 0.93(5)$ ), and oxygenated at high  $T_O$  (689 °C,  $\delta \approx 0.77(5)$ ). To avoid variations in the oxygenation value in these samples, once they reached the desired experimental conditions ( $t_{Oxyg} = 1 \text{ hr at } T_O$ ), they were rapidly (less than 1 s) brought to room temperature (below 30 °C), thus nullifying

oxygen diffusion in their structure[8].

Prior to each TGA measurement, and also X-ray measurements, a cleaning and deoxygenation ramp of the material was always performed. The temperature profile was as follows: Starting inside the TGA from normal ambient pressure, temperature, and humidity conditions, it was heated to 900 °C at 10 °C/min in a N<sub>2</sub> atmosphere. Then, these conditions were maintained at 900 °C for 30 min. Then, it was lowered to 30 °C at -10 °C/min in a N<sub>2</sub> atmosphere. Then, these conditions were maintained at 30 °C for 10 min. Then, it was heated to the T<sub>O</sub> (between 320 °C and 790 °C) at 10 °C/min in a N<sub>2</sub> atmosphere. Then, these conditions were maintained at the T<sub>O</sub> for 1 hr. Finally, the oxygenation experiments were began by changing the atmosphere from N<sub>2</sub> to O<sub>2</sub> under identical temperature (T<sub>O</sub>) conditions and maintaining this state for 1 hr to collect the data presented in this work. Once the aforementioned oxygenation process was completed, the system was always cooled to 30 °C at -10 °C/min while maintaining the O<sub>2</sub> atmosphere. In this post-acquisition process, it was confirmed that temperature variation in the O<sub>2</sub> atmosphere affects the oxygenation value[8], reinforcing the decision to have performed a rapid temperature cooling (quench) on the samples measured by X-rays. For some particular T<sub>O</sub> where saturation of the mass value was not observed during the standard oxygenation process (T<sub>O</sub> less than 450 °C), t<sub>Oxyg</sub> was extended upon to 5 hours.

The initial step of this ramp, heating to 900 °C and subsequent cooling to 30 °C in a N<sub>2</sub> atmosphere, was designed to remove impurities such as moisture acquired during grinding or remnants of oxide material that may have remained in the shaping process. We thus assume that our material starts with a heating ramp from 30 °C (approximately room temperature) to T<sub>O</sub> in pure state (100% YBCO) and in a condition of complete deoxygenation ( $\delta = 0$ ). The N<sub>2</sub> atmosphere accompanying this last heating allows the material to remain deoxygenated until reaching the T<sub>O</sub>. The plateau of 1 hs at the T<sub>O</sub> and under inert atmosphere conditions prior to the Oxygenation process allows the system to stabilize and rid itself of any error or uncertainty in the measurement arising from possible artifacts inherent in the measurement equipment under those conditions. The change of atmosphere to the T<sub>O</sub> is done without gas mixing outside the controlled system, where each gas enters the TGA through separate channels. The decision to work with powder material allows maximizing the contact surface of O<sub>2</sub> with the material, also minimizing the volume of material away from the surface. Thus, effects of variation in the Oxygen composition of the sample or any other edge effect from

working with samples where Oxygen diffusion plays an important role in its pathway to the material's interior are discarded. In this way, we assume that Oxygenation is homogeneous throughout the volume of the material.

### III. RESULTS

The Fig. 1 provides the evolution of relative masses  $m/m_{(\delta=0)}$  for the different  $T_O$  values studied, as a function of  $t_{Oxyg}$ . In it,  $m$  represents the sample mass, and  $m_{(\delta=0)}$  represents the mass of the fully deoxygenated sample. The theoretical mass value corresponding to the maximum possible Oxygenation,  $\delta = 1$ , is marked as a reference on the graph. Other  $\delta$  values are also marked as references:  $\delta = 0.3$ ,  $\delta = 0.5$ , and  $\delta = 0.63$ [2, 5, 6, 8, 10]. The sample mass clearly increases as a function of exposure time in an Oxygen-saturated atmosphere, which we directly associate with the material's degree of Oxygenation. The rate at which the material saturates its degree of Oxygenation, as well as the saturation value it reaches, clearly depend on the  $T_O$  value. The results shown are for  $t_{(Oxyg)} < 1$  hs for all the  $T_O$  values studied. We note that, for  $T_O$  values below 450 °C, for the displayed  $t_{Oxyg}$ , the sample mass continues to evolve without reaching a final stabilization value. For  $T_O$  values above 500 °C, the system is observed to reach saturation in this mentioned  $t_{Oxyg}$  time.

In line with this, three samples with different degrees of Oxygenation were studied by X-ray experiments. One sample under conditions of  $\delta = 0$  ( $t_{Oxyg} = 0$ ), and two samples Oxygenated for 1 hour at  $T_O = 350$  °C ( $\delta \approx 0.93(5)$ ) and at  $T_O = 689$  °C ( $\delta \approx 0.77(5)$ ). For the deoxygenated sample, a Tetragonal structure was observed, while for both Oxygenated samples, an Orthorhombic structure was observed. This corresponds to literature data, where the structural T-O transition is expected to occur at  $\delta$  values beyond 0.63 ( $0.5 \leq \delta \leq 0.63$ )[2].

Observing the saturation times in the Fig. 1 for the different  $T_O$  values studied, we make an initial comparison of the Oxygenation values reached in short and long times. We arbitrarily take 5 minutes and one hour (or more) as references, respectively. The Fig. 2 provides the value reached by the relative mass increase  $m/m_{(\delta=0)}$  at 5 minutes of the Oxygenation process starting (red diamonds) and at oxygen saturation of the material (blue circles) for each of the  $T_O$  values studied. As mentioned earlier, for low  $T_O$  values (below 450 °C),  $t_{Oxyg}$  was extended to over an hour to achieve saturation. It is observed that for some

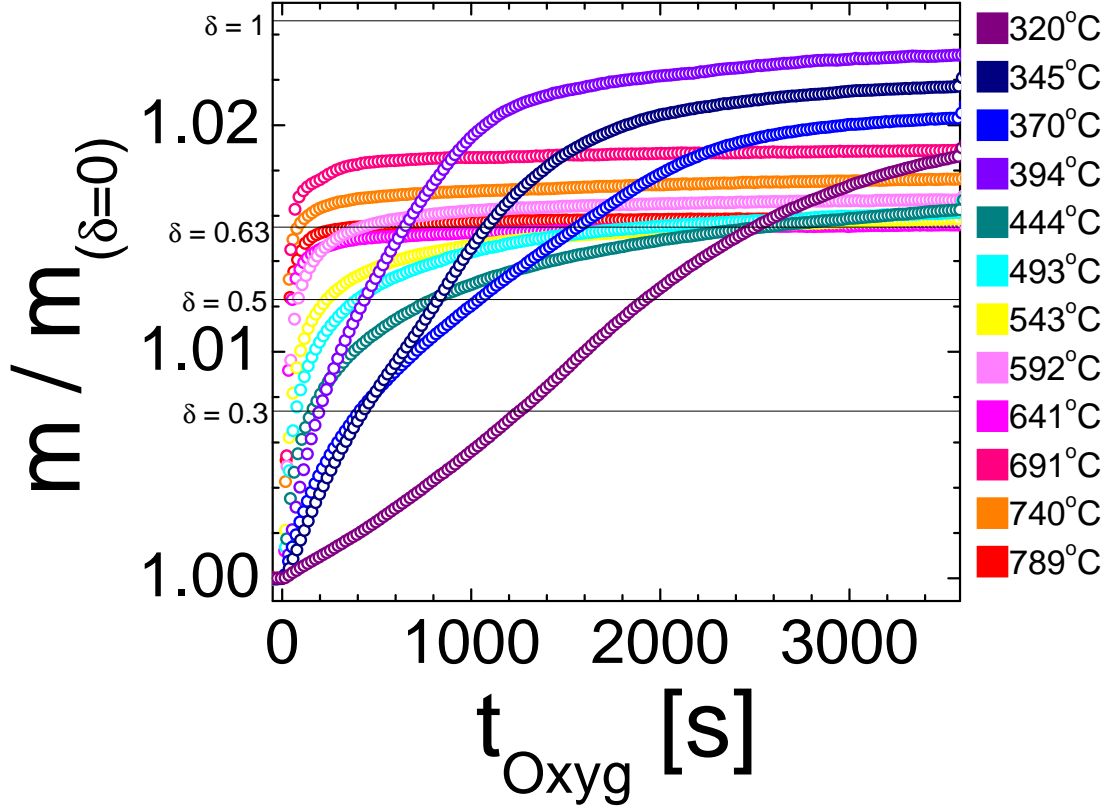


FIG. 1. Evolution at constant  $T_O$  of relative mass with respect to  $t_{Oxyg}$ , for different values of  $T_O$  ranging from 320 °C to 789 °C. Here,  $m$  represents the measured mass and  $m_{(\delta=0)}$  the mass of the material when fully deoxygenated. Various oxygenation values  $\delta$  are indicated as references on the  $m/m_{(\delta=0)}$  scale ( $\delta = 1$ ,  $\delta = 0.63$ ,  $\delta = 0.5$ , and  $\delta = 0.3$ ). A growth in mass with respect to  $t_{Oxyg}$  is observed. Additionally, both the rate of mass growth and the final saturated value depend on the  $T_O$  value. It is also noted that the system continues to evolve for  $T_O$  values below 450 °C within the range of shown  $t_{Oxyg}$  ( $t_{Oxyg} < 1$  hr).

$T_O$  values, the saturation value reached is very close to the value corresponding to  $\delta = 1$ , reinforcing the hypothesis of considering the sample fully deoxygenated at the beginning of the Oxygenation experiments. The maximum Oxygenation value at saturation is observed for  $T_O = 394$  °C and corresponds to a  $\delta$  value of 0.97. Then, for  $T_O$  above 600 °C, we note that the difference between the Oxygenation values reached at  $t_{Oxyg} = 5$  minutes and for saturation values is minimal (below the 5%), observing a maximum in Oxygenation around 690 °C.

On the other hand, and parallel with the mass evolution, we observe the DTA results

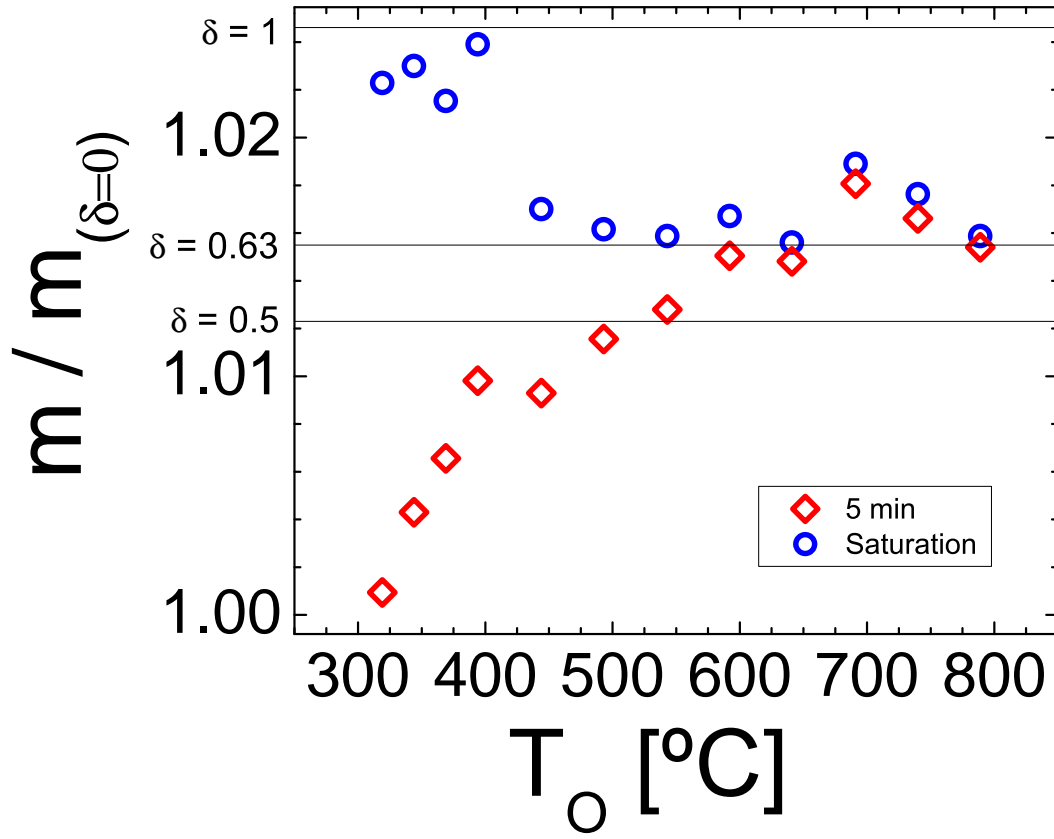


FIG. 2. Measured value in oxygenation experiments at constant  $T_O$  of relative mass  $m/m_{(\delta=0)}$  as a function of  $T_O$ . Values are shown for  $t_{Oxyg} = 5$  min (red diamonds) and at saturation condition for  $t_{Oxyg} \geq 1$  hs (blue circles). It is observed that, despite obtaining higher oxygenation values at low temperatures, above 600 °C an oxygenation value of the material near to the saturation is reached in very short times.

yielded by the experiment. The DTA corresponds to the measurement of a differential thermocouple between sample and reference. The Fig. 3 shows the DTA value as a function of  $t_{Oxyg}$  for each of the  $T_O$  values studied. The data are shown on a double logarithmic scale where, for better observation, for each  $T_O$ , the graph has been shifted a fixed value upwards and to the right relative to the immediately preceding  $T_O$  value. Data for  $T_O = 320$  °C corresponds, with no shifting, to the axis pair shown on the graph. It is observed that the Oxygenation process is clearly exothermic, with a clear increase in temperature relative to the reference. A first peak, which above 450 °C becomes the predominant effect of the curves, is associated with this phenomenon. Furthermore, we can observe a second

peak that for high  $T_O$  is practically drawn as a shoulder in the curves, while for low  $T_O$ , it takes on the relevance of the first peak corresponding to the Oxygenation process. This second peak is indicated in the curves with an arrow, and we associate it with an imprint of the T-O transition present in the material. The position of this second peak is obtained by fitting the drop of the first peak with a double exponential function and subtracting that value from the curve.

The Fig. 4 shows the location in  $t_{Oxyg}$  times of the two peaks observed for each of the curves, as a function of  $T_O$ . The peak associated with the material's Oxygenation process is indicated in black, and the peak associated with the T-O transition is indicated in red.

From the times shown in the Fig. 4 for which peaks we associate with the material's T-O transition appear, and taking up the mass evolution as a function of  $t_{Oxyg}$  (Fig. 1), for each of the  $T_O$  value we can associate the T-O transition with a specific  $\delta$  value. The Fig. 5 provides the detail of the Fig. 1 for low  $t_{Oxyg}$  values, adding the positions of the observed T-O transition's peak for each  $T_O$  data set. The left graph shows the mass evolution for the first 30 minutes of the Oxygenation process, while the right graph focuses on the first almost 5 minutes of the experiment (320 s). Arrows indicate the positions of the second peak observed by DTA, which we associate with the T-O transition, and can be referenced here with the material's degree of Oxygenation  $\delta$ .

At first glance, it is observed that, in general, all peaks fall within the Oxygenation range  $0.5 \leq \delta \leq 0.63$ , despite some exceptions for very low or very high  $T_O$  values[2]. To better interpret these variations and discrepancies, we plot the position of the peak associated with the T-O transition in a graph of  $T_O$  value as a function of  $\delta$ . The Fig. 6 shows this result. It shows, in red circles, positions of peaks associated with the T-O transition measured by DTA in this work. As a reference, dashed blue lines show the values of the T-O transition proposed from first-principles calculations obtained using a 2D-ASYNNNI model[6]. T denotes the Tetragonal phase, O-I denotes the Ortho-I superstructure, and O-II denotes the Ortho-II superstructure. The black dotted lines are only drawn as a guide to the eye.

It is observed that, in principle, the measured values at low  $T_O$  are in good agreement with the theoretical line separating the O-II superstructure from the T phase and the O-I superstructure. However, we note that these data are located at temperatures slightly above the theoretical predictions[7, 8]. For temperatures greater than 400 °C, the data measured in this work agree with the theoretical prediction for the T-O transition (O-I

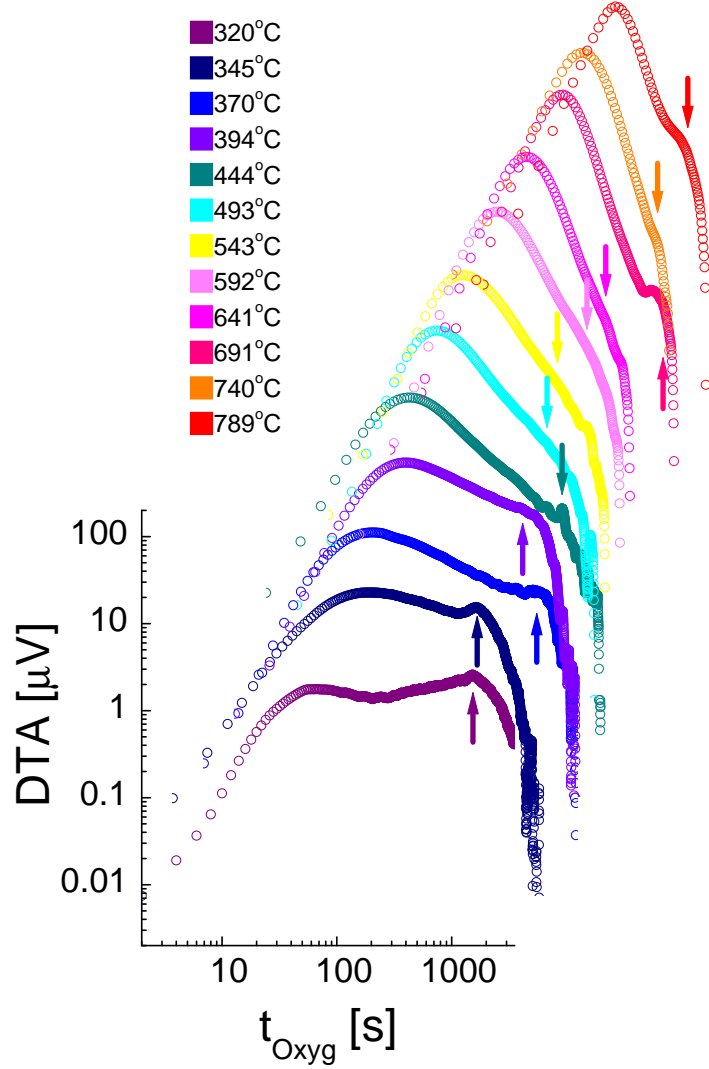


FIG. 3. DTA signal of the material during the oxygenation process at constant  $T_O$ , as a function of  $t_{Oxyg}$  and for different values of  $T_O$  in the range from 320 °C to 789 °C. The temperature during the oxygenation process of an inert sample (alumina powder) is taken as a reference. The data is shown on a double logarithmic scale. Data for the lowest  $T_O$  value corresponds to the axis pair shown on the graph. For a better observation, data corresponds to any other  $T_O$  value has been shifted a fixed value upwards and to the right relative to the immediately preceding  $T_O$  value data set. Two exothermic processes are observed during the material oxygenation. The first, predominant at high temperatures, corresponds to the oxygenation of the material. The second, indicated by arrows in the curves, is associated with the T-O transition present in the material.

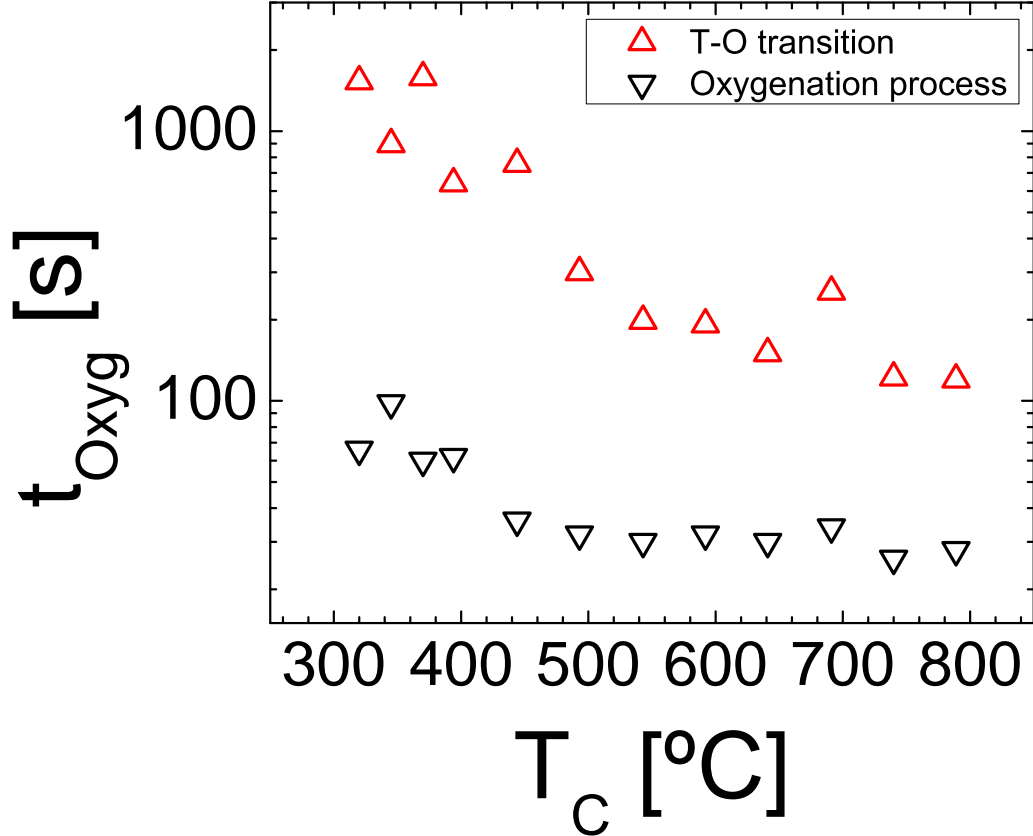


FIG. 4. Values of  $t_{Oxyg}$  corresponding to peak positions observed at DTA measurements performed at constant  $T_O$ , as a function of  $T_O$ . The graph shows peaks associated with the oxygenation process in black and peaks associated with T-O transition in red. It is observed that, in general, for every  $T_C$  worked peaks are separated by an order of magnitude in  $t_{Oxyg}$  (measured in seconds).

superstructure)[7, 8].

#### IV. CONCLUSIONS

We observed that the thermal cycling ramp in an inert atmosphere proposed and employed prior to the TGA experiments is effective for cleaning and deoxygenating the superconducting YBCO powder material. It was also confirmed that the hypothesis of starting from a completely deoxygenated sample ( $\delta = 0$ ) is correct.

Regarding the diffusion rate of  $O_2$  in the material, we noticed higher efficiency in the oxidation process for  $T_O$  values above 600 °C; where, for practical purposes, an oxidation

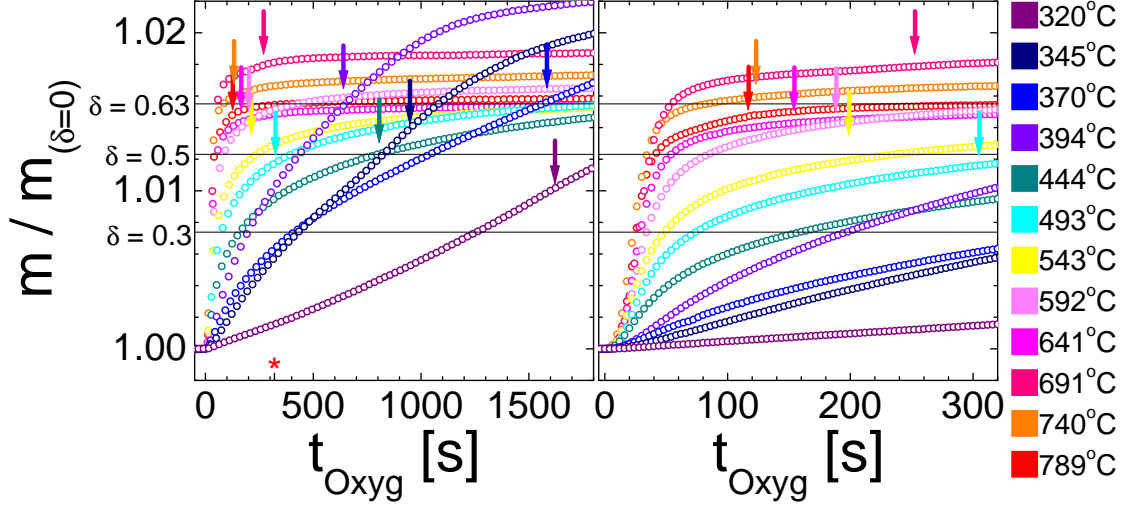


FIG. 5. Evolution at constant  $T_O$  of relative mass with respect to  $t_{Oxyg}$ , for different values of  $T_O$  in the range from 320 °C to 789 °C. Figures show the detail of the Fig. 1 for low values of  $t_{Oxyg}$ . The positions of the second maxima observed by DTA and associated with the T-O transition in the material are indicated with arrows. The figure on the right shows the data at low values of  $t_{Oxyg}$  from the left figure (from the origin to the red asterisk) for a better appreciation of the data at high  $T_O$  values. It is observed that, despite finding most of the peaks in the range of  $0.5 < \delta < 0.63$  in accordance with ref. [10], there are some discrepancies.

experiment with  $t_{Oxyg} = 5$  min yields the same results as an experiment with  $t_{Oxyg} = 1$  hr, within 5 % of tolerance. Particularly, we measured optimal oxidation under  $t_{Oxyg}$  minimization conditions for  $T_O$  around 691 °C. It is important to observe the speed at which these high values of  $\delta$  are reached, always in relation to the saturation value at the same temperature of  $T_O$ . We noticed that for  $T_O = 691$  °C, we measured a  $\delta$  value of  $\approx 0.73$  reached in just 5 minutes of  $t_{Oxyg}$ ; while for  $T_O = 394$  °C, we measured the same  $\delta$  value in less than 15 minutes of  $t_{Oxyg}$ . However, we should not consider  $t_{Oxyg}$  as a 1-3 ratio for these two values of  $T_O$ , but rather consider the rate at which the system saturates. For  $T_O$  of 691 °C, we measured saturation for  $t_{Oxyg}$  of 5 minutes, and for  $T_O$  of 394 °C, we measured saturation for  $t_{Oxyg}$  of 45 minutes, both within 5 % of tolerance. Therefore, in terms of saturation, we say that the relationship between  $t_{Oxyg}$  values for these two temperatures is 1-9, a value more related to the diffusion rate of  $O_2$  in the material.

Regarding the signature left by the T-O transition in TGA and DTA measurements,

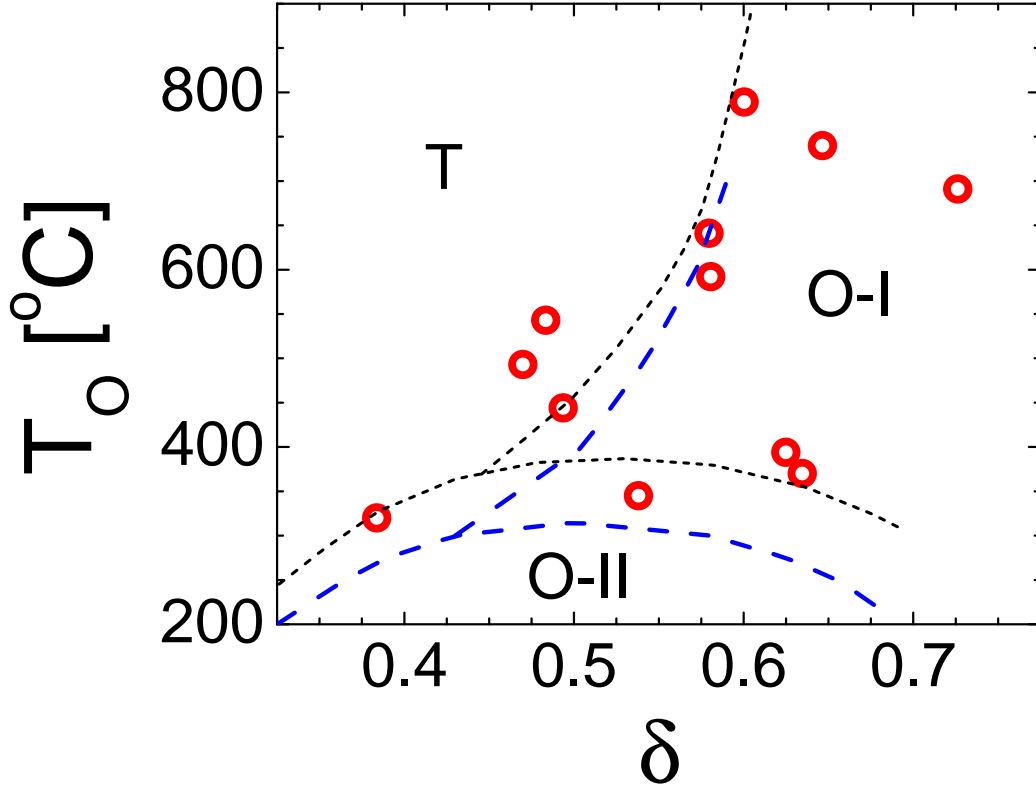


FIG. 6. Structural phase diagram of YBCO in a  $T_O$  vs.  $\delta$  graph, obtained from the position of the T-O transition observed in experiments of DTA for the oxygenation process at constant  $T_O$ . Measured data are shown as red circles. Values for the theoretically predicted structural phase diagram according to ref. [6] are shown as blue dashed lines. A shift towards higher temperatures of the measured data in this work compared to theoretical predictions in the literature is observed. This shift is indicated by black dotted lines as a guide to the eye.

its appearance is clear in the latter as it corresponds to an exothermic transition. On the other hand, a subtle change in concavity is observed in all curves in Fig. 5 at the moment of transitioning to the Orthorhombic phase. This indicates an increase in the rate of  $O_2$  absorption by the material due to the presence of the T-O transition. Thus, in coherence with the previous assertion, we assume that the material's T-O transition contributes to the Oxygen diffusion within it.

This topic has been widely discussed in bulk samples[11, 12]. Cracks in the material have been identified, which alter the Oxygenation dynamic. It is logical to assume that the

appearance of a mechanism (like cracks) that directly facilitates  $O_2$  diffusion in the material along the  $c$  axis aids on its diffusion. However, the cause of the appearance of such cracks is not considered in literature. Our results show an acceleration in  $O_2$  absorption associated with the T-O transition. We can say that, for bulk samples, on the material surface and at least up to a depth of  $2.5 \mu\text{m}$  (a radius associated with the grain size with which we work), our results demonstrate the presence of this phenomenon. Furthermore, the change in the lattice parameters  $a$  and  $b$  associated with the T-O transition produces an abrupt deformation in the  $a$ - $b$  plane of the crystal structure, elongating the system in the  $b$  direction and shortening it in the  $a$  direction[2]. In bulk samples, this abrupt deformation of the unit cell, if not accompanied by the entire system (at least 7 orders of magnitude larger than the dimensions of the unit cell for laboratory bulk samples[11, 12]), could cause the appearance of cracks. This, coupled with the significant structural difference that can occur with very small variations in Oxygen in the material[13], implies the need for high elasticity in the structure to prevent crack formation. This, evidently, is not present in bulk single crystal samples[11, 12]. We demonstrate in this work that it is not the appearance of cracks directly responsible for the change in the material's Oxygenation dynamics, but rather the intrinsic T-O transition of the material that leads to a sharp jump in the values of the unit cell parameters and consequently to the appearance of these so-called cracks on its surface.

Finally, based on the results obtained from the Oxygenation value of the material at which the peaks associated with the T-O transition appear, we draw the structural phase diagram of YBCO on a  $T_O$  vs.  $\delta$  graph. Our data delineate the interface between the T-O phases and the interface between the O-I and O-II superstructures. Initially, our results are in good agreement with predictions made using an Ising model with first-principles calculations (a 2D ASYNNNI model[6]) and agree with data obtained by measuring YBCO samples via neutron powder diffraction[7]. What stands out from the data measured in this work is that they delineate the boundary between the O-I and O-II superstructures. In previous experiments[6–8], the interface between this two superstructures has been observed only through experiments at constant  $\delta$ , that is, with temperature variation. Furthermore, in our case, since our experiments delineate the roof of the O-II superstructure's dome and we could approximate it by a region at constant  $T_O$ , we are surprised to be able to run along it and delineate it. We assume that the quantity of defects generated in the material's crystal structure when obtaining the YBCO powder allows the Tetragonal phase dabbles metastably

to much higher  $\delta$  values. We trust this only occurs at the interface between the O-I and O-II superstructures because the latter is a short-range order superstructure[8] allowing the disordered coexistence of many O-II nucleation centers, maintaining a Tetragonal structure in the material until the effective appearance of the Orthorhombic phase with long-range order (O-I)[8]. We thus propose that for our experiments, the trigger for the T-O transition is the exit from the O-II dome, transitioning to the O-I superstructure, which has long-range order.

On the other hand, Frello *et al.*[8, 14] performs high-energy X-ray diffraction experiments at low  $T_O$  values (below 200 °C), observing the interface between superstructures at these temperatures, i.e., 200 °C below what is predicted by theoretical models[6, 8]. In a subsequent study, by performing calculations that also consider 3D interaction terms as an extension of the 2D ASYNNNI model[9], he justifies the appearance of the interface between O-I and O-II superstructures for  $T_O$  around 100 °C, claiming very high purity of their samples. In our case, the method used to obtain the YBCO powder with which we work, mechanical milling using an agate mortar, can most likely introduce defects such as dislocations, inclusion planes, or any other type of structural defects into the material. This could even explain the appearance of the roof of the O-II superstructure approximately 50 °C above what is theoretically proposed[6]. More over, for regions of the O-II superstructure dome at lower temperatures (below those studied in this work), it is difficult to know what could effectively trigger the transition from the Tetragonal phase to the Orthorhombic phase. Under these conditions, the O-II dome widens, and the difference in  $\delta$  between the Tetragonal and the long-range order Orthorhombic phase O-I superstructure is expected to be of the order of  $\Delta\delta = 0.4$  or higher. The same pressure from O-II nucleation centers could even induce the T-O transition when still inside the O-II superstructure dome. In our experiments we assume it would appear as the emergence of a third peak, a new one in between the peak of oxigenation and the peak of the transition to the long-range order O-I superstructure.

However, considering that the Tetragonal phase advances within the Orthorhombic zone of the material only in the presence of a short-range order superstructure (O-II), metastability should not occur for temperatures above 400 °C, where the Orthorhombic phase is purely long-range order (O-I). In that sense, the appearance of metastability in this transition for the data measured and shown here at  $T_O = 691$  °C is puzzling. We rule out that this is

due to the appearance of other superstructures already measured in the material (O-III, O-V, O-VIII or even O-II) as these occur at lower temperature values[8]. Despite this, it is also noteworthy that for  $T_O$  values above 600 °C, the T-O transition occurs for  $\delta$  values in coherence with the material's Oxygen saturation value. Additionally, saturation rates for  $T_O$  values above 600 °C are not only the highest but also similar to each other (difference in the m value for the  $t_{Oxyg}$  shown in Fig. 2). We observed that for these  $T_O$  values, Oxygen saturation occurs at very short times, and the final values of  $\delta$  reached maintain a proportional relationship with the  $\delta$  values at which the T-O transition occurs. This indicates that the metastability at these  $T_O$  values depends not only on defects but also on the abrupt rates (for structural changes) at which oxidation occurs. Considering this possibility, we propose that metastability of the Tetragonal phase at these higher  $T_O$  values (incursing into the O-I superstructure) and under our experimental conditions, occurs due to the violent oxygenation rate. We understand it could be useful for confirming this assertion, to extend these studies by conducting oxidation experiments at lower rates, as we notice that this could bring the measured results of the T-O transition closer to the theoretically predicted line (Fig. 6). For experimental techniques we have access in our laboratories, it was not possible to perform such experiments since a partially saturated  $O_2$  atmosphere implies working with a mixture of both gases ( $N_2$  and  $O_2$ ), driving the experiment unstable and noisy.

## V. FINAL REMARKS

From YBCO powder obtained by mechanical milling of superconducting pellets, both mass evolution and the value of the relative temperature referenced to an inert sample were studied as functions of the oxidation time. Starting from completely deoxygenated samples, a maximum oxidation of  $\delta = 0.97$  was achieved for  $T_O = 394$  °C. It was also observed that, for short times,  $t_{Oxyg} = 5$  min, the material reaches maximum oxidation for  $T_O = 691$  °C, saturating within 5 % of tolerance in the m value. Additionally, the values of differential thermometry indicated the oxidation process as an exothermic type. It was also observed that, associated with this process, there is a second exothermic process, which we link to the T-O transition in the material. Both processes were well-differentiated from each other, appearing one order of magnitude apart in a  $t_{Oxyg}$  scale measured in units of seconds. Subsequently, a  $\delta$  value was associated with the T-O transition for each  $T_O$ . With these values, a

structural phase diagram for the material was constructed, observing not only the T-O phase transition but also the interface between O-I and O-II superstructures in the Orthorhombic phase. Finally, based on variations of our results compared to theoretical models predicting the structural phase diagram of the material[6, 8], different mechanisms were proposed that generate metastability during the T-O transition in the oxidation process. On one hand, at low temperatures, a mechanism of multiple nucleation centers of a superstructure with short-range order (O-II) was proposed to maintain the metastability of the Tetragonal phase. On the other hand, at high temperatures, a mechanism where the high speed in the oxidation process plays a very important role was proposed. Both cases are accompanied by a significant density of structural defects intrinsic to the nature of the samples with which we work. In addition to this, the enormous potential of a thermogravimetry setup combined with *in-situ* differential thermal analysis was highlighted. With these simple and accessible results, it was possible to replicate results previously obtained in large facilities using techniques such as neutron diffraction and high-energy X-ray diffraction[14].

## VI. ACKNOWLEDGMENTS

This work was partially supported by MINCyT through the PICT-2017-2898 FONCyT project. LG performed the TGA-DTA experiments and oxygenation analysis. CES performed the YBCO pellet growth and X-ray experiments and analysis. JAM contributed to the YBCO pellet growth, TGA-DTA experiments and X-ray experiments. RFL performed the TGA-DTA experiments and structural transition analysis, conducted the research and wrote out the manuscript. All authors contributed equally to discussion of ideas and correction of the manuscript.

- 
- [1] J. R. Waldram, Superconductivity of Metals and Cuprates, Taylor & Francis Group, 1996. doi:doi:<https://doi.org/10.1201/9780203737934>.
- [2] P. K. Gallagher, H. M. O'Bryan, S. A. Sunshine, D. W. Murphy, Oxygen stoichiometry in  $\text{YBa}_2\text{Cu}_3\text{O}_x$ , Materials Research Bulletin 22 (1987) 995. doi:doi:[https://doi.org/10.1016/0025-5408\(87\)90099-7](https://doi.org/10.1016/0025-5408(87)90099-7).

- [3] M. O. Eatough, D. S. Ginley, B. Morosin, E. L. Venturini, Orthorhombic-tetragonal phase transition in high-temperature superconductor  $\text{YBa}_2\text{Cu}_3\text{O}_7$ , *Applied Physics Letter* 51 (1987) 367. doi:doi:https://doi.org/10.1063/1.98443.
- [4] W. I. F. David, W. T. A. Harrison, J. M. F. Gunn, O. Moze, A. K. Soper, P. Day, J. D. Jorgensen, D. G. Hinks, M. A. Beno, L. Soderholm, D. W. C. II, I. K. Schuller, C. U. Segre, K. Zhang, J. D. Grace, Structure and crystal chemistry of the high-*t<sub>c</sub>* superconductor  $\text{YBa}_2\text{Cu}_3\text{O}_{7-x}$ , *Nature* 327 (1987) 310. doi:doi:https://doi.org/10.1038/327310a0.
- [5] H. M. O'Bryan, P. K. Gallagher, Characterization of  $\text{Ba}_2\text{YCu}_3\text{O}_x$  as a function of oxygen partial pressure. part ii: Dependence of the o-t transition on oxygen content, *Advanced Ceramic Materials* 2 (1987) 640. doi:doi:https://doi.org/10.1111/j.1551-2916.1987.tb00129.x.
- [6] G. Ceder, M. Asta, W. C. Carter, M. Kraitchman, D. de Fontaine, Phase diagram and low-temperature behavior of oxygen ordering in  $\text{YBa}_2\text{Cu}_3\text{O}_z$  using *ab initio* interactions, *Physical Review B* 41 (1990) 8698. doi:doi:https://doi.org/10.1103/PhysRevB.41.8698.
- [7] N. H. Andersen, B. Lebech, H. F. Poulsen, The structural phase diagram and oxygen equilibrium partial pressure of  $\text{YBa}_2\text{Cu}_3\text{O}_{6+x}$  studied by neutron powder diffraction and gas volumetry, *Physica C* 172 (1990) 31. doi:doi:https://doi.org/10.1016/0921-4534(90)90639-V.
- [8] M. v. Zimmermann, J. R. Schneider, T. Frello, N. H. Andersen, J. Madsen, M. Käll, H. F. Poulsen, R. Liang, P. Dosanjh, W. N. Hardy, Oxygen-ordering superstructures in underdoped  $\text{YBa}_2\text{Cu}_3\text{O}_{6+x}$  studied by hard x-ray diffraction, *Physical Review B* 68 (2003) 104515. doi:doi:https://doi.org/10.1103/PhysRevB.68.104515.
- [9] N. H. Andersen, M. v. Zimmermann, T. Frello, M. Käll, D. Mønster, P. A. Lindgård, J. Madsen, T. Niemöller, H. F. Poulsen, O. Schmidt, J. R. Schneider, T. Wolf, P. Dosanjh, R. Liang, W. N. Hardy, Superstructure formation and the structural phase diagram of  $\text{YBa}_2\text{Cu}_3\text{O}_{6+x}$ , *Physica C* 317 (1999) 259. doi:doi:https://doi.org/10.1016/S0921-4534(99)00066-0.
- [10] P. K. Gallagher, Characterization of  $\text{Ba}_2\text{YCu}_3\text{O}_x$  as a function of oxygen partial pressure. part i: Thermoanalytical measurements, *Advanced Ceramic Materials* 2 (1987) 632. doi:doi:https://doi.org/10.1111/j.1551-2916.1987.tb00128.x.
- [11] P. Diko, M. Kaňuchová, X. Chaud, P. Odier, X. Granados, X. Obradors, Oxygenation mechanism of TSMG YBCO bulk superconductor, *Journal of Physics: Conference Series* 97 (2008) 012160. doi:doi:https://doi.org/10.1088/1742-6596/97/1/012160.

- [12] P. Diko, X. Granados, B. Bozzo, P. Kulík, Oxygenation thermogravimetry of TSMG YBCO bulk superconductor, *EEE Transactions on Applied Superconductivity* 17 (2007) 2961. doi:doi:  
<https://doi.org/10.1109/TASC.2007.898219>.
- [13] R. Beyers, B. T. Ahn, G. Gorman, V. Y. Lee, S. S. P. Parkin, M. L. Ramirez, K. P. Roche, J. E. Vazquez, T. M. Gur, R. A. Huggins, Oxygen ordering, phase separation and the 60-K and 90-K plateaus in  $\text{YBa}_2\text{Cu}_3\text{O}_x$ , *Nature* 340 (1989) 619. doi:doi:<https://doi.org/10.1038/340619a0>.
- [14] T. Frello, Structural and superconducting properties of High- $T_C$  superconductors, Ph.D. thesis, Risø National Laboratory, Roskilde, Denmark, 1999. ISBN: 87-550-2476-9; 87-550-2477-7 (internet).